INSTITUTE OF PLASMA PHYSICS

NAGOYA UNIVERSITY

RESEARCH REPORT

NAGOYA, JAPAN

ELECTRON HEATING AND ANOMALOUS TRANSPORT IN THE INITIAL STAGE OF TURBULENT HEATING OF A PLASMA

H. Iguchi

IPPJ-299

Aug. 1977

Further communication about this report is to be sent to the Research Information Center, Institute of Plasma Physics, Nagoya University, Nagoya 464, Japan.

ABSTRACT

Initial stage of a linear turbulent heating of a plasma has been investigated by use of Thomson scattering of ruby laser light with an eight channel polychromator. In a low density discharge ($n \simeq 5 \times 10^{12}$ cm^{-3}), an anomalously rapid electron heating was observed associated with the appearance of high frequency fluctuations ($\omega \lesssim \omega_{pi}$), which were considered to be current driven ion acoustic waves. Flat-top velocity distribution of the electrons were also observed just after the onset of the ion acoustic instability. Formation of this flat-top distribution was interpreted as a quasilinear diffusion process in velocity space in the presence of ion acoustic waves. In a high density discharge ($n \simeq 2 \times 10^{14}$ cm^{-3}), it was found that the skin current distribution was rapidly destroyed, while skin profile of the radial distribution of the electron temperature remained rather longer, indicating that the plasma current redistributed without electron heat transfer across the magnetic field. The anomalous resistivity caused by ion acoustic waves was essential for the anomalously rapid current penetration.

1. INTRODUCTION

Since the first experiment by M. V. Babykin et al.,[1] many authors have studied the turbulent heating of a plasma in both linear and toroidal devices. In these studies electrons and ions with a density of $10^{11} \sim 10^{14}$ cm^{-3} were heated up to 1 ∿ 10 keV within one microsecond,[2] and the effectiveness of this method for heating of plasmas was demonstrated. The mechanism of this heating of a plasma has been interpreted as the dissipation of the directional energy of the current in the presence of current instabilities such as an ion acoustic instability and a Buneman instability. Especially the electron heating has been explained by "an anomalous ohmic heating" associated with the anomalous resistivity caused by these current instabilities. In these experiments, the electron temperature has been measured by X-ray spectroscopy,[3] diamangetic loops[4] and so on, but the temporal and spatial evolution of the electron temperature in the initial stage of the heating discharge, which might play the most important role to determine the microscopic turbulent state, has not been measured in detail.[5]

In this paper, we present an experimental investigation of the initial stage of a linear turbulent heating of a plasma, where the measurement of the electroan temperature was performed by use of Thomson scattering of ruby laser light with an eight channel polychromator. In a low density discharge ($n \simeq 5 \times 10^{12}$ cm^{-3}), it was confirmed that; (1) anomalously rapid electron heating started when the ion acoustic instability was excited, and (2) the velocity dis-

tribution of the electrons in a plasma became flat-topped when the instability started to grow. In a high density discharge ($n \simeq 2 \times 10^{14}$ cm^{-3}), it was found that (3) the anomalously rapid penetration of a plasma current occurred without electron heat transfer across the magnetic field.

It has been suggested that an ion acoustic instability and resultant anomalous resistivity are responsible for the rapid electron heating in turbulent heating of a plasma. However, as mentioned above, the process of the onset of this instability and the rapid electron heating were not clarified. To our knowledge there has been no experiment which has confirmed the correspondence of them in a high current turbulent heating discharge.

In a turbulent plasma, wave-particle interactions are quite strong and distortion of the velocity distribution of electrons and ions from Maxwellian has been expected. Since the phase velocity of ion acoustic waves in the plasma is less than the thermal velocity of plasma electrons and larger than that of plasma ions, the enhanced diffusion in velocity space is expected to bring a flat-top velocity distribution of the electrons and hot tail of ions. Experimentally many authors have reported the formation of hot tails[6] in the velocity distribution of ions in turbulent heating of a plasma, while the flat-top distribution of electrons has not been reported except computor simulations.[7]

An anomalously rapid disappearance of a current skin has been observed not only in turbulent heating discharges but in tokamak discharges. This has motivated a study of

many micro-instabilities that could cause rapid penetration of a plasma current, though most of them have not been experimentally confirmed. In some turbulent heating experiments in low density discharges ($n \lesssim 1 \times 10^{13}$ cm^{-3}), the anomalous skin effect was explained in terms of the anomalous resistivity[8], or the anomalous viscosity[9]. However a lack of information about the radial profile of the electron temperature has so far prevented further progress of the study of the anomalous skin effect. Especially in high density plasmas there were few experiments on this problem. Our measurements of radial profile of the electron temperature as well as plasma current in the skin phase led us to go into detail discussions about the anomalous skin effect.

In Sec.2 experimental apparatus and methods are described. The experimental results on a low density discharge and on a high density discharge are shown in Sec.3.1 and Sec.3.2, respectively. Section 4 is devoted to discussions of the electron heating (Sec.4.1), the flat-top velocity distribution of the electrons (Sec.4.2) and the anomalous skin effect (Sec.4.3). Finally concluding remarks are summarized in Sec.5.

2. EXPERIMENTAL APPARATUS

2.1 THE MACH II Device

This experiment was carried out by use of THE MACH II device[10] (Fig.1). A vacuum vessel of Pyrex glass having an inner diameter of 17 cm and a length of about 2 m was placed in ten series-connected solenoid coils. In the case of a

low density discharge a hydrogen plasma was produced and injected into the vessel by a titanium washer gun, and in the case of a high density discharge a helium plasma was produced by a conical theta pinch gun. The magnetic field strength was 15 kG except the region of a diagnostic port (7.5 kG). Two hollow electrodes for the heating discharge, made of aluminum with inner and outer diameter of 3 and 4.5 cm, respectively, were placed in the vessel separated from each other by 135 cm. The electrode voltage and current for heating discharge were obtained from two series-connected capacitors of 2.2 μF each, with charging voltages up to 15 kV to give 1.1 μF at 30 kV. The heating current wave form was produced by an overdamped discharge through nonlinear resistors which was connected in series in the discharge circuit. A half period of the discharge current was determined mainly by the inductance of the external circuit ($L \simeq 2 \times 10^{-6}$ H) and was about 5 microseconds. In these circumstances, $\omega L \sim \sqrt{L/C} \sim 1.4\Omega$, while the resistance of the plasma column before the heating discharge was about 0.02Ω in the case of a low density discharge and about 0.1Ω in the case of a high density discharge. Then only a small fraction of the charged voltage of the capacitor was applied to the plasma column at the intstance when the discharge circuit was closed, and high energy runaway electrons could be avoided in the early stage of the heating discharge. These situations are different from the usual toroidal turbulent heating experiment and some of linear ones. The voltage between two electrodes and the current for heating discharge

were measured with a voltage divider and with a Rogowski coil surrounding the plasma column, respectively, and the resistance of the plasma column was computed from these values, taking into account the net inductance of the circuit.

Fluctuations in the plasma with a frequency range up to 500 MHz were measured by use of a floating double probe (copper wires of 0.5 mm diameter, 3 mm length, and 2 mm separation). Signals were transmitted through a coaxial cable and a 1/100 attenuator to a high speed oscilloscope. Current distributions were measured by use of a five channel magnetic probe. Five coils were aligned with one centimeter separation and mounted in an insulating glass tube of 6 mm diameter.

2.2 The Thomson Scattering Apparatus

The optical system for laser scattering is also shown in Fig.1. The ruby laser beam, having an energy of 10 J and a pulse width of 20 nsec, was introduced at a right angle to the axis of the plasma column, and was focused at the center by a converging lens (focal length 60 cm). Light scattered at 90° to the direction of the incident beam was collected by a 10 cm diameter lens placed at 40 cm from the observed point and it was imaged onto the entrance slit of the spectrometer. Spatial scanning along the incident beam was made by rotating a mirror placed just below the collecting lens. Spectrum of the scattered light was analyzed by a spectrometer 25 cm, f/4.5, with 1200/mm grating, which gave a dispersion of 30 Å/mm. The spectrometer output was coupled to

8 photomultiplier tubes by fibre optics light guides. The time resolution of the meesurements was about 50 nsec.

Relative calibration of the channels was made by use of a calibrated tungsten filament lamp (W-lamp). Light emmitted from the W-lamp was introduced through a photo-chopper and imaged on the entrance slit of the spectrometer and relative intensity of the signals was recorded as a calibration factor. For the estimation of a statistical error $1/\sqrt{N}$, where N is the number of photoelectrons collected per channel, we measured the scattered light from the initial plasma about 30 times. From these data it was determined that the statistical error was about 10 % for the output signal of 50 mV in our experimental set up.

The scattering parameter α is given by $\alpha = \lambda_o/4\pi\lambda_D \sin(\theta/2)$ where λ_o is a wavelength of the incident light, λ_D is the Debye length and θ is a scattering angle. In our experimental conditions, $\alpha < 0.01$ in the case of a low density discharge, and $\alpha < 0.1$ in a high density discharge. So the spectrum of the scattered light had information of random electron motion, that is, the velocity distribution function of the electrons. If the velocity distribution is Maxwellian, the spectrum is Gaussian and full width at half maximum is given by $\Delta\lambda(\mathring{A}) = 32.6\sqrt{T_e(eV)}$.

3. EXPERIMENTAL RESULTS

3.1 Low Density Discharge[11]

First we describe the experimental results on a low density discharge with a hydrogen plasma produced by a

titanium washer gun. The electron density at the center of the diagnostic port was measured by laser scattering method and is shown in Fig.2, where t_o is the time when the gun was fired. It was shown that the electron density was about 5×10^{12} cm^{-3} and its axial inhomogeneity between two electrodes was estimated to be less than 50 % when the turbulent heating discharge was fired at $t - t_o = 70$ μsec. The diameter of the plasma column was about 3 cm. Typical wave forms of the voltage between two electrodes and the heating current are shown in Fig.3. We note that the heating current increased monotonically for about 1 μsec while the voltage remained low. After 1.0 ∿ 1.2 μsec the voltage increased rapidly and the current saturated and dipped, that is, the plasma showed high resistance. The scattering measurement was made throughout the heating discharge, where the scattered light was viewed from the volume having dimensions 1 mm × 5 mm × 20 mm.

Temporal evolution of the spectrum of the scattered light is shown in Fig.4. Each spectrum was obtained by statistical average of several shots and the error bars mean statistical error of $1/\sqrt{N}$, where N was total photo-electrons of the several shots collected at each channel. The time t was measured from the time of the initiation of the heating current. Before the onset of the heating discharge, the velocity distribution of the electrons in the plasma was Maxwellian and the temperature was about 8 eV. During the first 0.6 μsec of the discharge, the electron temperature T_e increased slowly. From t ∿ 0.6 μsec T_e started to rise faster and then the velocity distribution departed from

Maxwellian and became rather flat-topped with an effective temperature $T_e^{eff} = \langle mv^2 \rangle$ of about 20 eV at t ∿ 0.8 μsec. The resistance of the plasma column until t ∿ 0.8 μsec was much less than 1 Ω. Rapid electron heating started at t = 0.9 ∿ 1.0 μsec and immediately scattered light signals disappeared behind the plasma radiations, coincident with an abrupt increase of the resistance of the plasma column (3 Ω).

Other measurements of electron temperature by X-ray spectroscopy, diamagnetic loops[10] and microwave scattering[12] from ion acoustic waves indicated that the electron temperature reached to higher than several kiloelectronvolts at t = 1.5 ∿ 1.7 μsec when the resistance of the plasma column was maximum.

Typical oscillogram of the output signals of a floating double probe are shown in Fig.5. The observed potential fluctuations were divided into two types: One was observed immediately when the heating current started and has frequency of a few MHz, and another began to be observed at t = 0.6 ∿ 0.8 μsec having frequency of 100 ∿ 400 MHz. We refer the former type A fluctuations and the latter type B fluctuations. Type B fluctuations started to grow at t = 0.6 ∿ 0.8 μsec and its amplitude reached maximum when the resistance of the plasma column became maximum.

Figure 6 shows the typical results of the temporal development of (a) the heating discharge current, (b) the computed resistance of the plasma column from $V_H - I_H$ characteristics, (c) the electron temperature, and (d) the amplitude of the type B fluctuations. From these figures,

the onset of anomalously rapid electron heating and the appearance and growth of the type B fluctuations were found to be coincident well. Furthermore, the resistance of the plasma column and the amplitude of the fluctuations were also strongly correlated.

3.2 High Density Discharge[13]

Turbulent heating was applied to a helium plasma produced by a conical theta pinch gun. A radial profile of the electron density before the heating discharge was measured by use of an electrical double probe and is shown in Fig.7(a), and full width at half maximum of it was about 4 cm. The electron density of about 2×10^{14} cm^{-3} on the axis of the plasma column was obtained by laser scattering method, and the electron temperature before the heating discharge was $1 \sim 2$ eV. In this case the voltage between the two electrodes was less than a few kilovolts throughout the discharge, though the charging voltage of the capacitor of 36 kV and the total current of about 8 kA were almost the same as the low density discharge. Scattering experiment was performed at several radial positions with spatial resolution of 4 mm in radial direction.

Typical results of the measurements of the azimuthal magnetic field B_θ produced by the plasma current are shown in Fig.7(b). Each data point was obtained from a statistical average of several shots. The time resolution of the measurements was about 0.1 μsec. Our data point outside r = 4 cm did not depart much from 1/r dependence, which indicated

that the current channel remained mostly within r = 4 cm. The current reached to the axis of the plasma column within 0.6 μsec, and increased with a shape of cylindrical-symmetry though a little radial shift of the current channel was observed. At t = 1.8 ∿ 2.0 μsec, low frequency oscillations (≲ 1 MHz) of B_θ appeared, which seemed to be closely related to a magnetohydrodynamic instability, but we do not go into details here.

Temporal development of the electron temperature at each radial position from r = 0.0 to 2.0 cm is shown in Fig.8. Each data point with error bars means a statistical average and one standard deviation of several shots. The error bars in time axis mean the time of the measurements were within these regions. Dotted lines are the temporal development of the electron temperature in the case of an ohmic heating with Spitzer resistivity, which were calculated from the observed current density assuming that the electron density and its profile did not change. Energy loss and heat convection were neglected and the effective charge of the ions was assumed to be one. In fact, the electron density within r = 2.0 cm did not change appreciably during the interval of the measurements. Before t ∿ 0.8 μsec the heating rate for the electrons at each radial position (r = 2.0 cm) was of the order of what was due to the ohmic heating with Spitzer resistivity. Anomalously rapid electron heating started from the periphery of the plasma column and penetrated into the axis. It should be noted that appreciable time delay of the onset of the anomalously rapid electron heating was ob-

served near the plasma core ($r \lesssim 1.0$ cm), while the rapid electron heating started at almost the same time ($t \sim 0.8$ μsec) in the layer outside $r = 1.0$ cm. These differences seem to be an indication that the electron thermal concuductivity in radial direction is different between the plasma core and the outer region.

Radial distribution of the current density and electron temperature at different instants of time are shown in Fig.9 which were deduced from Fig.7(b) and Fig.8. In the figure of $t = 1.2$ μsec, the point $r = 0$ corresponds to $r = -0.7$ cm (see Fig.7(b)) only for the measured current distribution. Dotted lines are the current density profile in a cylindrical conductor with the same radius and electrical resistivity as the initial plasma column. If we take into account the electron heating by an ohmic process, the resistivity of the plasma decreases and sharper skin profile is obtained. It was found that the skin current profile was rapidly destroyed while the electron temperature remained at a sharp skin profile near the plasma core, and the anomality of the current penetration was larger after the current reached to the axis of the plasma column. These facts indicate that the plasma current redistributed without electron heat transfer across the magnetic field in this high density region.

4. DISCUSSIONS

4.1 Fluctuations and Heating Rate of the Electrons

We discuss about the type B fluctuations and the heating rate of the electrons. From Fig.6(d) we can see that the

type B fluctuations were started to be observed at t = 0.6 $\sim$ 0.8 μsec, when the ratio of v_d/v_e became 0.5 $\sim$ 1.0 and T_e/T_i was about 2, where v_d and v_e were a drift velocity and a thermal velocity of electrons in the plasma, respectively. The amplitude of the fluctuations grew exponentially and saturated at t = 1.2 $\sim$ 1.7 μsec, when the resistance of the plasma column became maximum. The frequency of the fluctuations was in a region just below the ion plasma frequency (500 MHz). From these values (the critical drift velocity, the temperature ratio of electrons and ions and the observed frequency), the type B fluctuations seem to be current driven ion acoustic waves* with a phase velocity of $c_s = \sqrt{T_e/m_i}$.

The growth rate of this instability was deduced from Fig.6(d) and it was $\gamma \sim (5 \sim 10) \times 10^6$ sec^{-1}, which was a little smaller than the linear growth rate of the ion acoustic instability, $\gamma \sim (\pi/8)^{1/2}(m_e/m_i)^{1/2}\omega_{pi} \sim 3 \times 10^7$ sec^{-1}. Some damping mechanisms such as collisional damping, ion Landau damping and other nonlinear effects seem to influence the growth of the waves. One of the most important effects is, the quasilinear effect, that is, the deformation of the velocity distribution of the electrons from a drifted Maxwellian in parallel direction. Observed flat-top velocity distribution seems to be an indication of this effect, which will be discussed in the next subsection.

The electron heating is closely related to the resis-

---

* Recently the type B fluctuations were studied in detail by a microwave scattering method[12] and a capacitive probe,[14] and they were identified as ion acoustic waves propagating nearly perpendicular to the magnetic field.

tivity of a plasma. From Fig.6(c) we can see that $dT_e/dt \sim 1 \times 10^7$ eV/sec in the first 0.6 μsec. Introducing the effective electron-ion collision frequency ν_H responsible for electron heating as

$$\frac{3}{2}\frac{dT_e}{dt} = \frac{1}{2} m_e v_d^2 \nu_H$$

we obtain $\nu_H \sim 2 \times 10^6$ sec^{-1}. The electron ion collision frequency ν_{ei} for a quiet plasma at the initial electron temperature was about 7×10^6 sec^{-1} and of the order of ν_H, which indicated that the electron heating at $t \lesssim 0.6$ μsec is explained by ohmic heating with Spitzer resistivity. The anomalously rapid electron heating started at $t \sim 0.6$ μsec, and during the period of $t = 0.9 \sim 1.6$ μsec the heating rate became about 5×10^9 eV/sec. From this value we obtain $\nu_H \sim 1 \times 10^8$ sec^{-1} or larger if we take into account heat losses due to the thermal conduction. The second effective collision frequency ν_R was deduced directly from the resistivity measured from the $V_H - I_H$ characteristics of the heating discharge. The resistance of the plasma column at $t = 1.0 \sim 1.2$ μsec was one ohm or less, so that we obtain $\nu_R \lesssim 3 \times 10^8$ sec^{-1} assuming the uniform turbulence in axial direction, which was larger than ν_{ei} in this period by several orders. The two values, ν_H and ν_R are in good agreement within the experimental error during the period of the anomalously rapid electron heating. It can be concluded that the anomalously rapid electron heating is attributed to "an anomalous ohmic heating" due to the anomalous resistivity caused by the ion acoustic instability.

For the current driven ion acoustic instability, the effective collision frequency was proposed by Sagdeev[15] as

$$\nu_s = \frac{1}{10^2} \frac{v_d}{c_s} \frac{T_e}{T_i} \omega_{pi}$$

which was deduced from Kadomtsev's spectra $I(k) \sim k^{-3} \ell nk^{-1}$. During the period of fast electron heating, substituting the value $v_d/v_s \sim 10$, $T_e/T_i \sim 10$, we obtain $\nu_s \sim 3 \times 10^9$ sec^{-1}. This value is larger than the previous two effective collision frequency by an order of magnitude. Thoeretically speaking, ν_s is valid when the fully developed ion acoustic turbulence exist, where the excitation of the waves by the current and nonlinear Landau damping are balanced. As the growth rate and damping rate of the ion acoustic instability depend on the electron temperature, it may not be possible to attain a fully developed steady state turbulence when the electron temperature is varying very rapidly in time. Actually turbulence level of W/nT_e (W: wave energy) is estimated from the semi-empirical formula

$$\nu_{eff} \simeq \frac{W}{n T_e} \omega_{pe}$$

with the help of the measured value of the anomalous resistivity and it is about 2×10^{-3}, which is rather small.

4.2 Flat-Top Velocity Distribution of the Electrons

From Fig.4 and Fig.6, the flat-top distribution appeared when the ion acoustic instability started to grow, and the half width of the flat-top region was about 10 eV at t = 0.8 μsec. This value is close to either the thermal energy or

the drift energy of the electrons at this time. Both low frequency and high frequency fluctuations observed by the floating double probe were not so strong that the observed flat-top distribution cannot be attributed to the spatial superposition of locally drifted Maxwellians due to E × B drift. To explain the observed width of the flat-top region by E × B drift $v_E = E_\perp(k)/B$, it is necessary that $v_E \simeq 3 \times 10^8$ cm/sec, which requires perpendicular electric field $E_\perp(k)$ of 20 kV/cm for the given magnetic field (7.5 kG). This value is unreal in this stage of the discharge. It is also clear that spatial superposition of different local temperatures cannot lead to the flat-top distribution. From these facts, the flattening of the distribution seems to be due to the quasilinear wave-particle interactions in the plasma during the course of the turbulent heating discharge.

According to quasilinear theory, the diffusion equation in velocity space is given as

$$\frac{\partial}{\partial t} f(v,t) = \frac{\partial}{\partial v} \cdot \left[\mathbb{D}(v,t) \cdot \frac{\partial}{\partial v} f(v,t) \right]$$

where $\mathbb{D}(v, t)$ is the diffusion tensor. Sagdeev and Galeev[16] calculated the asymptotic velocity distribution function of the electrons in the presence of a two-dimensional wave packet that has cylindrical symmetry in k space. They showed that final velocity distribution f(v) doesn't depend on the initial distribution and has the form of $f(v) \propto \exp(-v^5)$ outside the circle $v = \omega/k$ in velocity space, which appears like a flat-top distribution. In our experiment, v_d is close to v_e and much larger than c_s, and then if we assume

that ion acoustic waves excited by the electron drift is propagating almost perpendicular to the magnetic field, the phase velocity parallel to the magnetic field can be of the order of v_d. In this case the waves can interact with the main body of the electron distribution, where we assume the drifted Maxwellian of the electrons, which is not unreal in this stage of the discharge. These experimental conditions are similar to the situations assumed in the calculation by Sagdeev and Geleev. The computer simulation done by Birkamp, Chodura, and Dum[7] also showed the appearance of a flat-top distribution, $f(v) \propto \exp(-v^x)$ with $x = 3.6 \sim 4.0$, in the case of the current driven ion acoustic instability. Their time for the formation of the flat-top distribution was about 100 times the ion plasma period. Its appearance reduced the growth of the instability but did not limit it. These characters also don't contradict our experimental results.

Another explanation was proposed by Sugihara.[17] In the presence of a magnetic field, in addition to the resonance at $k_{\parallel}v_z - \omega_k = 0$, there is a resonance at harmonics of the cyclotron frequency, $k_{\parallel}v_z - \omega_k - n\omega_{ce} = 0$, where $k_{\parallel}$ and ω_{ce} are parallel component of the wave vector k and the electron cyclotron frequency, respectively and n is an arbitrary number. In this case the cyclotron motion of the electrons plays essential role in the process of the diffusion in velocity space, which is quite different from the theory of Sagdeev and Galeev. The kinetic equation in the presence of a magnetic field is given by

$$\frac{\partial f}{\partial t} + v \cdot \frac{\partial f}{\partial r} - \frac{e}{m_e}\left[\delta E + \frac{1}{c} v \times B_0\right] \cdot \frac{\partial f}{\partial v} = 0$$

where δE is the fluctuating electric field and B_0 is the static magnetic field. Separating f into the slowly varying part and the fast varying part as

$$f(r, v, t) = f_0(v_\perp^2, v_\parallel, t) + \sum_k \delta f_k(v, t) \exp\left[i(k_\perp x + k_\parallel z - \omega t)\right]$$

and following the quasilinear scheme, we have the velocity space diffusion coefficient in the perpendicular direction $D_\perp$;

$$D_\perp = \frac{\pi e^2}{m_e^2} \sum_{k,n} \left(\frac{n\omega_{ce}}{k_\perp v_\perp}\right)^2 J_n\left(\frac{k_\perp v_\perp}{\omega_{ce}}\right) \left|\delta E_\perp(k)\right|^2 \delta\left(k_\parallel v_z - \omega_k - n\omega_{ce}\right)$$

where J_n is the n-th Bessel function and $v_\perp$ is the perpendicular velocity component of the electrons. In $D_\perp$, the terms for $n = \pm 1$ will be dominant and $\delta(k_\parallel v_z - \omega_k - n\omega_{ce})$ is approximated by $\delta(k_\parallel v_z \pm \omega_{ce})$ because of $\omega_{ce} >> \omega_k$, where ω_k is the frequency of the ion acoustic waves ($\sim 10^9$ rad/sec) and $\omega_{ce} \simeq 1.3 \times 10^{11}$ rad/sec. Assuming $k_\parallel \sim k_D \simeq 6 \times 10^2$ cm^{-1} and taking $v_d \simeq 2 \times 10^8$ cm/sec we can see that the resonance condition is satisfied in the experiment. The quantity $(\omega_{ce}/k_\perp v_\perp)^2 J_1^2(k_\perp v_\perp/\omega_{ce})$ has its maximum at $v_\perp = 0$, that is, for the smaller $v_\perp$ the more intense velocity-space diffusion occurs. In this case we assumed $k_\parallel \sim k_D$, that is, $k_\parallel > k_\perp$. This assumption is contrary to the assumption which is required to use Sagdeev's theory. Recent experiments on fluctuations[12,14] showed that $k_\parallel < k_\perp$ for ion acoustic waves during $t = 1.0 \sim 1.5$ μsec. It seems that

the former explanation is more realistic than the latter, though the relation $k_{\parallel} < k_{\perp}$ is not confirmed at about t = 0.8 μsec.

4.3 Anomalously Rapid Current Penetration

The electron-ion collision frequency ν_{ei} for the initial plasma was about 2×10^9 sec^{-1} (at the plasma core) and the frequency of the external electromagnetic field ω was 6.8×10^5 rad/sec. Then the plasma was collisional ($\omega << \nu_{ei}$) even near its boundary, and the collisional skin depth given by $\delta \sim (c/\omega_{pe})(2\nu_{ei}/\omega)^{1/2}$ was about 4 cm, so that the plasma current could penetrate into the plasma core. However, it would take more than 2 μsec for the current distribution to become almost flat (see the dotted lines in Fig.9). The collisional electron viscosity η_o can be neglected, because $\eta_o \sim 2n_eT_e/\omega_{ce}^2\tau_e \sim 5 \times 10^{-11}$ [g/cm sec] is too small to explain the observed current penetration, where τ_e is an electron self-collision time.

In our experiment the current distribution remained axisymmetry until its parabolic profile was formed, so that no MHD mode might play an important role in the skin phase and some microscopic instabilities should be invoked. Microinstabilities so far proposed in association with this problem are tabulated in the reference [18]. They are divided into two types; (1) current driven modes, which are driven directly by the plasma current and (2) gradient driven modes, which are driven by radial gradients of the plasma current or the electron temperature. In the case of the current

driven modes such as an ion acoustic instability and Buneman instability, onset of an anomalous resistivity enhances the penetration of a driving electromagnetic field, while in the case of the gradient driven modes such as a velocity shear instability and a drift wave instability driven by electron temperature gradient, enhancement of an electron viscosity makes the plasma current redistribute with radial particle diffusion or thermal convection.

The anomalous viscosity associated with the instabilities driven by the electron temperature gradient modes, both a low frequency drift mode and a high frequency ion acoustic mode, would not be essential. The low frequency drift mode ($\omega << \omega_{ci}$) would not grow in such a short interval as in turbulent heating discharge. The ion acoustic mode driven by electron temperature gradient needs fairly large temeprature gradient ($|\frac{dT_e}{dx}| > 200$ eV/cm for our plasma), for the excitation condition is $v_\theta \sim |dT_e/dx|/m_e\omega_{ce} > c_s$ where v_θ is the diamagnetic drift velocity by electron temperature gradient and ω_{ce} is the electron cyclotron frequency.

The threshold condition for the velocity shear instability in the fluid limit ($\omega > k_{\parallel}v_e$) is given by[19]

$$\left|\frac{1}{v_d}\frac{dv_d}{dx}\right| > \frac{4\omega_{pe}v_e}{c^2}\left(1+\frac{\omega_{pe}^2}{\omega_{ce}^2}\right)^{1/2}$$

and it becomes restrictive as the electron density increases. In our experimental conditions $\frac{1}{v_d}\frac{dv_d}{dx} > 0(1)$ [cm^{-1}] near the plasma core. A velocity shear instability in another limit ($\omega < k_{\parallel}v_e$) is excited when[20]

$$\left|\frac{1}{v_d}\frac{dv_d}{dx}\right| > \frac{\omega_{ce}}{\nu_e}\left(\frac{m_e T_i}{m_i T_e}\right)^{1/2}$$

This criterion is more restrictive than the above mode by one order of magnitude in our case. Taking into account the fact that the current distribution changed rapidly without electron heat transfer across the magnetic field, the enhancement of the electron viscosity, which might occur if the velocity shear modes dominated throughout the skin phase, would not be essential at least near the plasma core.

The ratio of the linear growth rate for the velocity shear mode in the fluid limit γ^J to the current driven ion acoustic mode γ^A is given by[18]

$$\gamma^J/\gamma^A = \left|\frac{1}{v_d}\frac{dv_d}{dx}\right| \frac{\nu_e}{\omega_{ce}}\left(1+\frac{\omega_{pe}^2}{\omega_{ce}^2}\right)^{-1/2}\left(\frac{m_i}{m_e}\right)^{1/2}$$

and in our experimental conditions $\gamma^J/\gamma^A \sim 10^{-2}\left|\frac{1}{v_d}\frac{dv_d}{dx}\right|$ in cgs units. Then if the current driven ion acoustic mode becomes unstable, it will dominate the velocity shear mode, and will be essential for the anomalous skin effect.

However this ratio is valid when $T_e/T_i \gg 1$. If T_e/T_i is not so large ion Landau damping reduces the growth rate of the ion acoustic mode, and the above ratio of γ^J/γ^A increases. As our plasma has diffuse boundary, that is, the electron density decreases toward the plasma periphery and the ratio of T_e/T_i is not so large in the initial stage, the velocity shear mode in the fluid limit may be possible to exist near the plasma boundary.

In our experiment, the rapid electron heating started from the periphery of the plasma column, which suggested that the onset of the anomalous resistivity had started from the periphery. Actually the drift velocity of the electrons $v_d(r,t)$, for instance $r = 1$ cm and $t = 0.8$ μsec, was about 4×10^6 cm/sec, which is several times as large as $c_s(r,t)$, and conditions for an ion acoustic instability is satisfied. In fact, high frequency fluctuations with frequency ranges of a few hundred MHz, where ion plasma frequency was 1.5 GHz at the plasma core, and with amplitude up to 1 volt were detected by use of a capacitive probe, though they were resolved neither temporary nor spatially in the present experimental condiitions. Details on the fluctuations in a turbulently heated plasma in THE MACH II will be published elsewhere.

In the present case time delay of the electron temperature penetration from the current penetration can be understood. The heating rate of the electrons is $\frac{1}{T_e}\frac{dT_e}{dt} \sim \frac{m_e v_d^2}{T_e}\nu_{eff} \sim (\frac{v_d}{v_e})^2\nu_{eff}$ while the rate of change of the current density can be derived from the generalized ohm's law and is $\frac{1}{J}\frac{dJ}{dt} \sim \nu_{eff}$ where ν_{eff} is the effective electron ion collision frequency. In the case of the ion acoustic instability, the drift velocity v_d is of the order of c_s, and then $\frac{1}{T_e}\frac{dT_e}{dt} \sim \frac{m_e}{m_i}\nu_{eff}$, which is smaller than $\frac{1}{J}\frac{dJ}{dt}$ by the factor m_e/m_i. These considerations are summarized in Table 1.

Recently Nishida et al.[21] reported that the anomalously rapid thermal transport across the magnetic field was observed in the skin phase of a toroidal turbulent heating

experiment. Our result is different from theirs. The reason seemed to be that no mode which propagate across the magnetic field was excited at least near the plasma core in our experimental conditions.

5. CONCLUSION

Initial stage of a linear turbulent heating of a plasma was investigated by use of Thomson scattering of ruby laser light with an eight channel polychromator. In a low density discharge ($n \simeq 5 \times 10^{12}$ cm^{-3}) following features were found:

(1) It was experimentally confirmed that an anomalously rapid electron heating started coincident with the onset of high frequency fluctuations ($\omega \lesssim \omega_{pi}$), which was considered as an ion acoustic waves. The heating rate of the electrons in this stage was well explained by an "anomalous ohmic heating" due to the anomalous resistivity associated with the ion acoustic waves.

(2) Flat-top velocity distributions of the electrons were observed associated with the appearance of the ion acoustic waves. Formation of this flat-top distribution was interpreted as a quasilinear diffusion process in velocity space in the presence of ion acoustic waves.

In a high density discharge ($n \simeq 2 \times 10^{14}$ cm^{-3}) it was found:

(3) Anomalously rapid disappearance of the current skin was observed, while skin profile of the electron temperature remained longer near the plasma core, indicating that the plasma current redistributed without electron heat

transfer across the magnetic field. Current driven ion acoustic mode seemed to be essential, but a velocity shear mode might possibly be excited near the plasma periphery.

ACKNOWLEDGEMENTS

The author would like to express his sincere thank to a number of people who have contributed to this work, especially Professor K. Takayama, the director of the Institute of Plasma Physics, Nagoya University who provided continuous encouragement, and Professor T. Kawabe of the University of Tsukuba who provided guidance and suggestions throughout the work. Professor K. Watanabe of Osaka University was kindly taking care of our group. Professor K. Muraoka of Kyushu University gave technical and theoretical guidances on the laser scattering method in plasma experiment. Dr. Sugihara provided theoretical informations and discussions. Professors. T. Oda, K. Adati and Drs. T. Kawamura, Y. Amagishi, K. Ishii, K. Kondo, A. Mase and Y. Ito also provided valuable discussions. Messrs. O. Mitarai and Y. Takita gave technical assistance for the experiment. Finally he would like to thank Dr. Y. Nakagawa and staffs of Asada Fundamental Research Laboratory of Kobe Steel Co. Ltd. for preparing the titanium plasma source.

This work has been carried out under the cooperative research program at the Institute of Plasma Physics, Nagoya University, Nagoya, Japan.

References

1) M. V. Babykin, P. P. Gavrin, E. K. Zavoiskii, L. I. Rudakov and V. A. Skoryupin, Sov. Phys. JETP 16, 295 (1963).

2) For example, E. K. Zavoiskii, B. A. Demidov, Yu. G. Kalinin, A. G. Plakhov, L. I. Rudakov, V. D. Skoryupin, G. E. Smolkin, A. V. Titov, S. D. Fanchenko, V. V. Shapkin and G. V. Sholin, Proc. Fourth Intern. Conf. Plasma Phys. and Controlled Nucl. Fusion Res., Madison, Wisconsin, 1971 (IAEA, Vienna, Austria, 1972) Vol.II, p.3.

3) Yoshinobu Matsukawa, Yoshiro Nakagawa and Kenji Watanabe, J. Phys. Soc. Jap. 24, 196 (1968).

4) M. V. Babykin, P. P. Gavrin, E. K. Zavoiskii, S. L. Nedseev, L. I. Rudakov and V. A. Skoryupin, Sov. Phys. JETP 25, 421 (1967).

5) A. W. deSilva, J. Fujita, T. Kawabe, K. Kondo and T. Uyama, Phys. Fluids 17, 1780 (1974).

6) C. Wharton, P. Korn, D. Prono, S. Robertson, P. Auer and C. T. Dum, Proc. Fourth Intern. Conf. Plasma Phys. and Controlled Nucl. Fusion Res., Madison, Wisconsin, 1971 (IAEA, Vienna, Austria, 1972) Vol.II, p.25.

7) C. T. Dum, R. Chodura and D. Biskamp, Phys. Rev. Lett. 32, 1231 (1974).

8) M. Ushio and T. Ishimura, J. Phys. Soc. Jap. 39, 1956 (1975).

9) A. Hirose, T. Kawabe and H. M. Skarsgard, Phys. Rev. Lett. 29, 1432 (1972).

10) Y. Nakagawa, M. Tanikawa, K. Watanabe, K. Adati, H. Iguchi, K. Ishii, Y. Ito, J. Jacquinot, T. Kawabe, T. Kawamura, K. Muraoka, T. Oda and R. Sugihara, Proc. Fifth Intern. Conf.

Plasma Phys. and Controlled Nucl. Fusion Res., Tokyo, 1974 (IAEA, Vienna, Austria, 1975) Vol.III, p.287.

11) K. Adati, H. Iguchi, Y. Ito, T. Kawabe, K. Kondo, O. Mitarai, K. Muraoka and R. Sugihara, Phys. Rev. Lett. 35, 280 (1975).

12) A. Mase, T. Tsukishima, H. Iguchi, Y. Ito and T. Kawabe, to be published.

13) H. Iguchi, Y. Ito, T. Kawabe and K. Muraoka, to be published.

14) to be published.

15) R. Z. Sagdeev, Advances in Plasma Physics, Vol.5. (John Wiley & Sons, New York, 1974) p.153.

16) R. Z. Sagdeev and A. A. Galeev, Nonlinear Plasma Theory (Benjamin, New York, 1969).

17) R. Sugihara, Ann. Rev. IPP Japan, Apr.1974/Mar.1975, p.56.

18) J. B. McBridge, H. H. Klein, R. N. Byrne and N. A. Krall, Nucl. Fusion 15, 393 (1975).

19) A. Hirose and I. Alexeff, Phys. Fluids 16, 1087 (1973).

20) C. W. Liu, Phys. Rev. Lett. 27, 1637 (1971).

21) Y. Nishida, A. Hirose and H. M. Skarsgard, Phys. Rev. Lett. 38, 653 (1977).

Figure Captions

Fig.1. Schematics of the experimental arrangement.

Fig.2. Temporal variations of the electron density at the center of the diagnostic port without the heating discharge. Here t_o is the time when the gun is fired.

Fig.3. Typical oscillogram of the voltage between two electrodes (V_H) and the heating current (I_H).

Fig.4. Temporal evolution of the spectrum of the scattered light.

Fig.5. Typical oscillograms of the fluctuations at (a) t = 0.2 $\sim$ 2.2 μsec (200 nsec/div.), (b) t $\leq$ 0.35 μsec (50 nsec/div.) and (c) t = 12. $\sim$ 1.4 μsec (20 nsec/div.).

Fig.6. Temporal development of (a) the heating current, (b) the computed resistance of the plasma column, (c) the electroan temperature and (d) the amplitude of the high frequency fluctuations ($\omega \lesssim \omega_{pi}$).

Fig.7. (a) Radial profile of the initial electron density at the diagnostic port. (b) $B_\theta(r,t)$ obtained from the magnetic probe data at several instants of time.

Fig.8. Temporal development of the electron temperature at different radial positions.

Fig.9. Radial distributions of the plasma current and the electron temperature at several instants of time. The dotted lines are the current distributions in cylindrical conductor with the same electrical conductivity and radius as the initial plasma column (arbitrary units).

Table I. Possible Mechanisms for Anomalously Rapid Current Penetration.

Instabilities	Mechanism	Plasma Core	Plasma Periphery
Buneman	Anomalous Resistivity	No	No
Current Driven Ion Acoustic		Possible	Possible
Velocity Shear for $\omega > k_{\parallel} v_e$	Anomaloud Viscosity	No	Possible
Velosity Shear for $\omega < k_{\parallel} v_e$		No	No
Ion Acoustic Mode Driven by Temperature Gradient for $\omega^* << k_{\parallel} v_e$		No	No
Large Temperature Gradient for $\omega^* >> k_{\parallel} v_e$		No	No
Drift Mode Driven by Temperature Gradient		No	No
MHD Mode	Reconnection of Magnetic Lines of Force	No	No

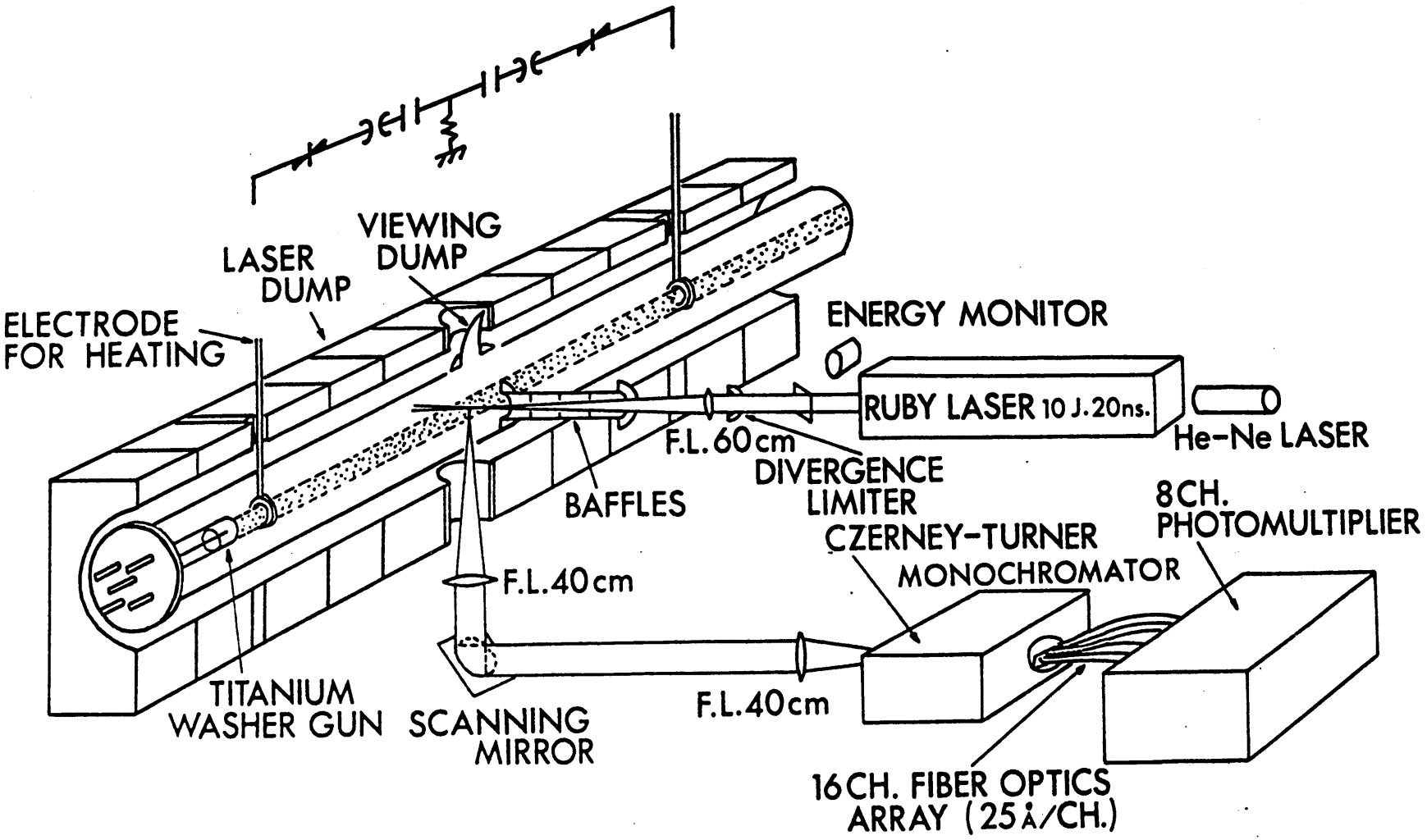
LASER DUMP
VIEWING DUMP
ELECTRODE FOR HEATING
ENERGY MONITOR
RUBY LASER 10 J. 20ns.
He-Ne LASER
F.L. 60cm
DIVERGENCE LIMITER
BAFFLES
8CH. PHOTOMULTIPLIER
CZERNEY-TURNER MONOCHROMATOR
F.L. 40cm
TITANIUM WASHER GUN
SCANNING MIRROR
F.L. 40cm
16CH. FIBER OPTICS ARRAY (25Å/CH.)

Fig. 1

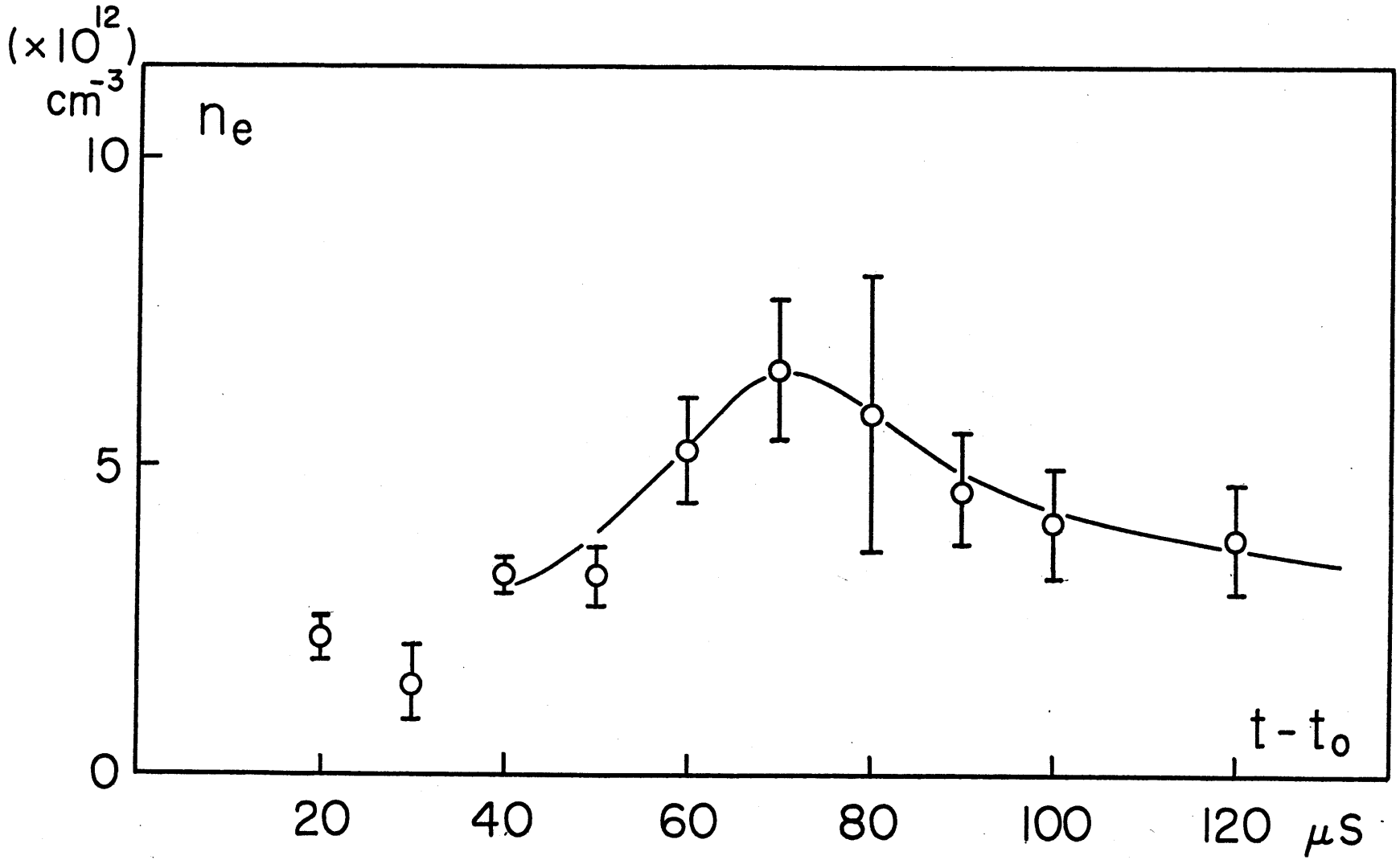

Fig. 2

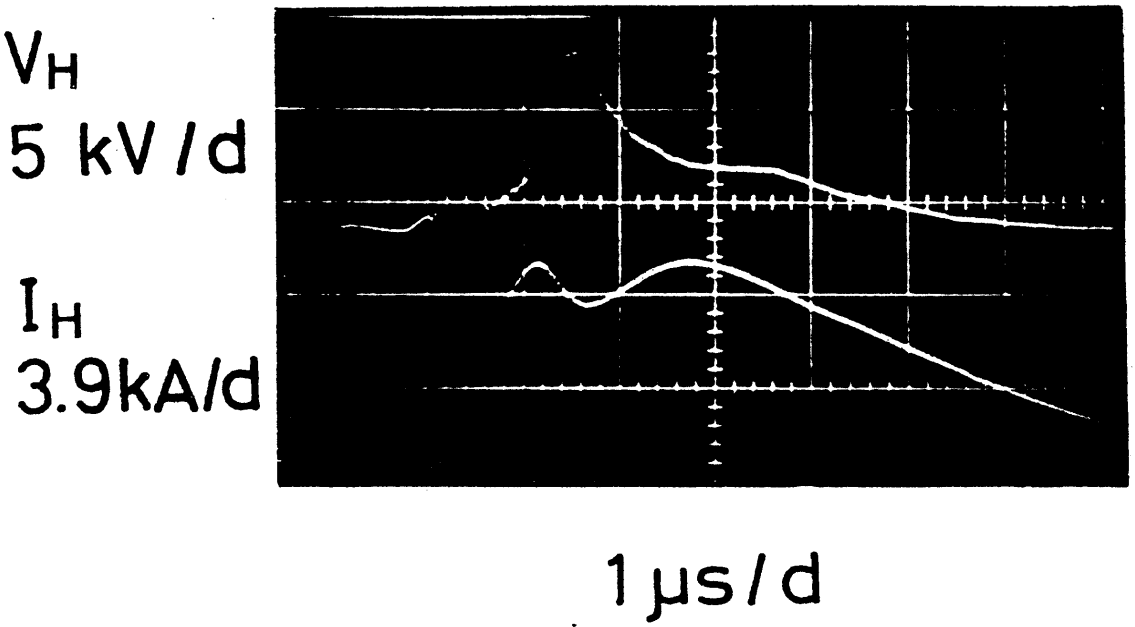

Fig. 3

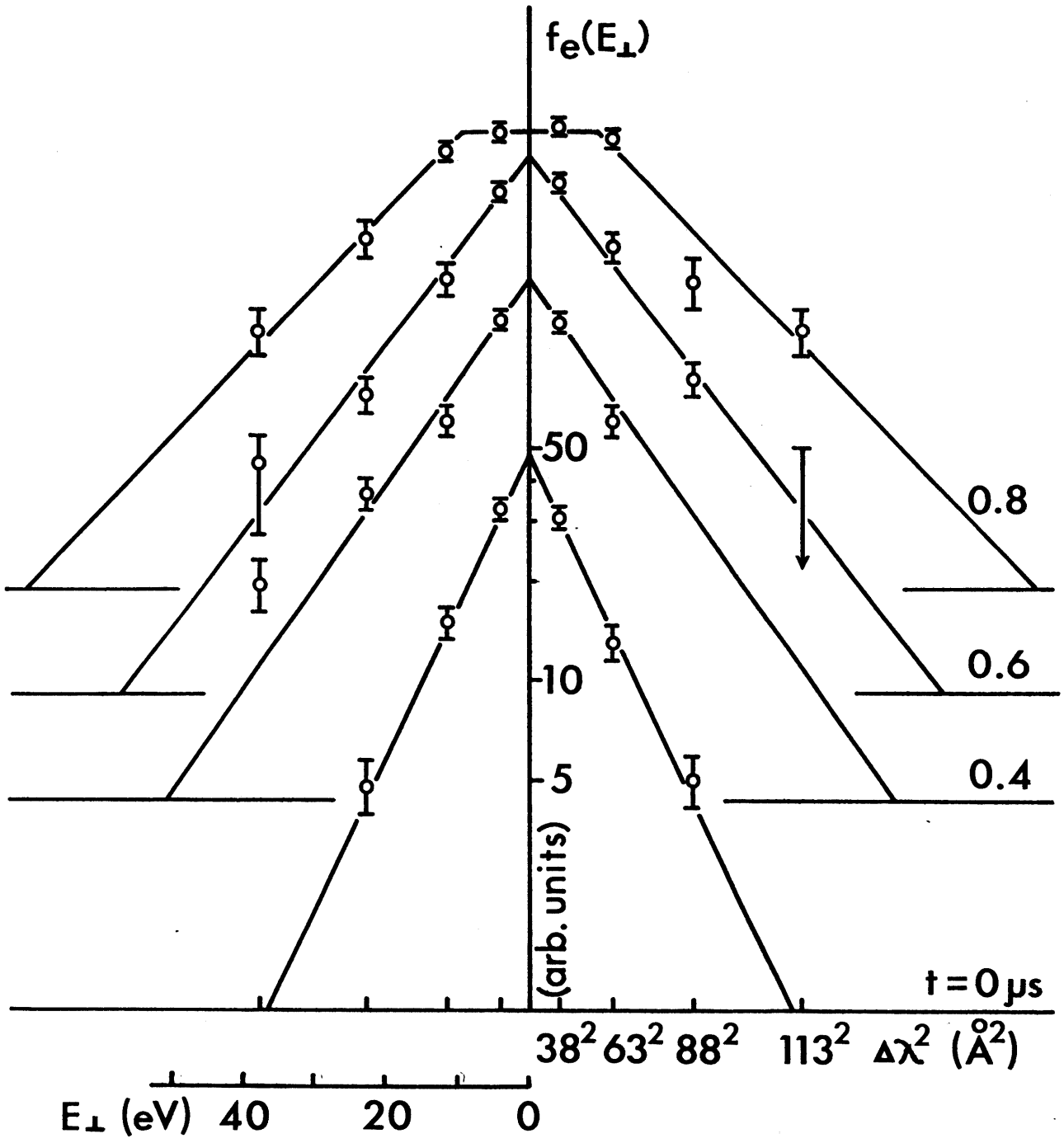
$f_e(E_\perp)$
50
10
5
(arb. units)
0.8
0.6
0.4
t = 0 μs
38^2 63^2 88^2 113^2 $\Delta\lambda^2$ ($Å^2$)
$E_\perp$ (eV) 40 20 0

Fig. 4

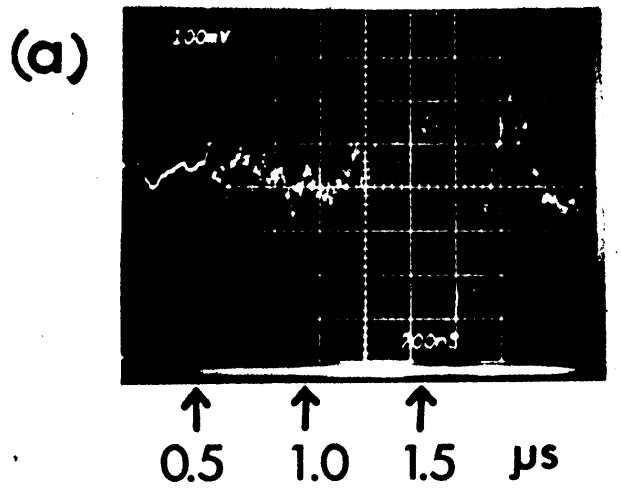

Fig. 5

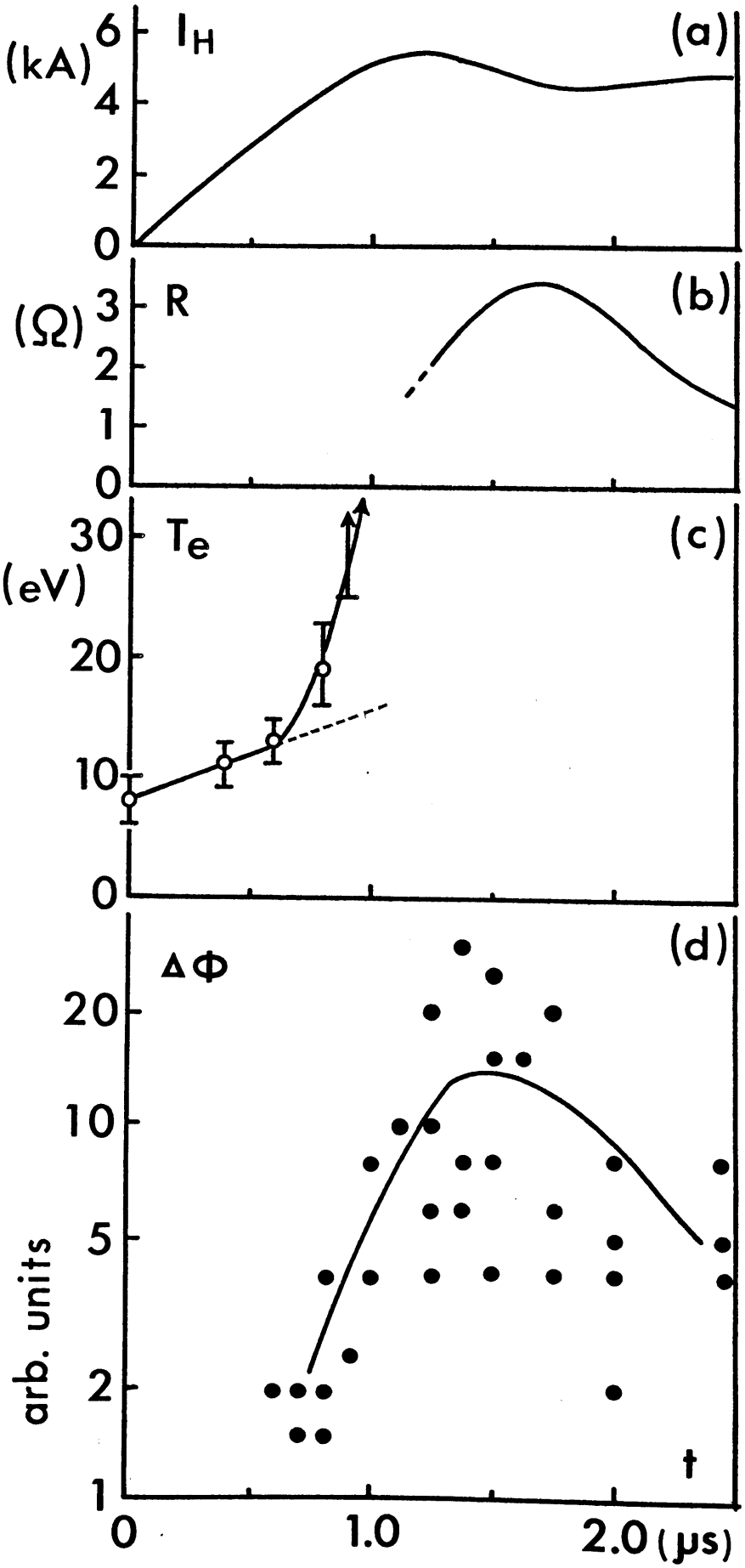
(kA)
6
4
2
0
I_H
(a)
(Ω)
3
2
1
0
R
(b)
30
20
10
0
(eV)
T_e
(c)
20
10
5
2
1
arb. units
ΔΦ
(d)
t
0
1.0
2.0 (μs)

Fig. 6

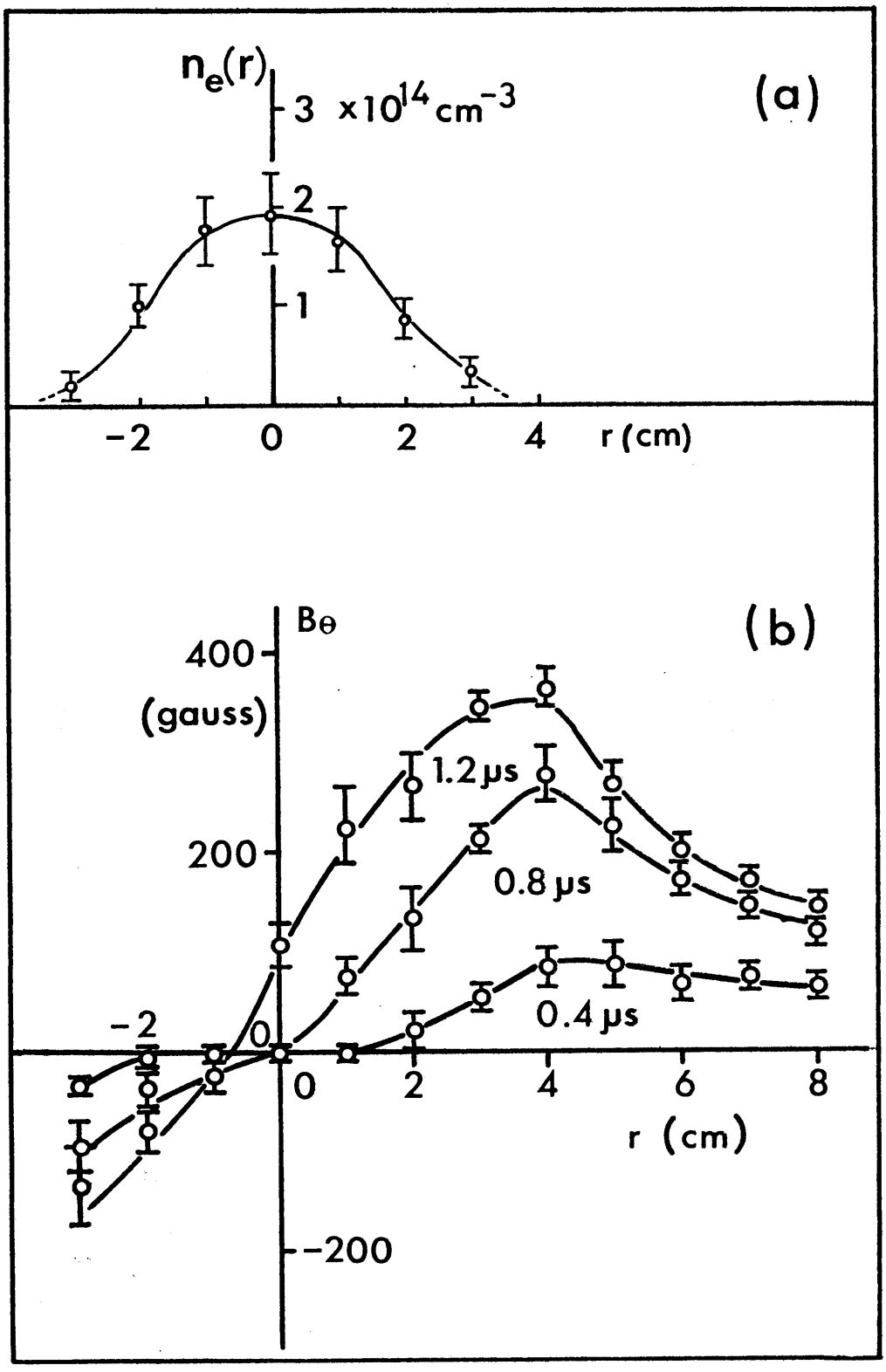
$n_e(r)$
3 x10^{14}cm^{-3}
(a)
2
1
-2
0
2
4
r (cm)
Bθ
(b)
400
(gauss)
1.2 μs
200
0.8 μs
0.4 μs
-2
0
0
2
4
6
8
r (cm)
-200

Fig. 7

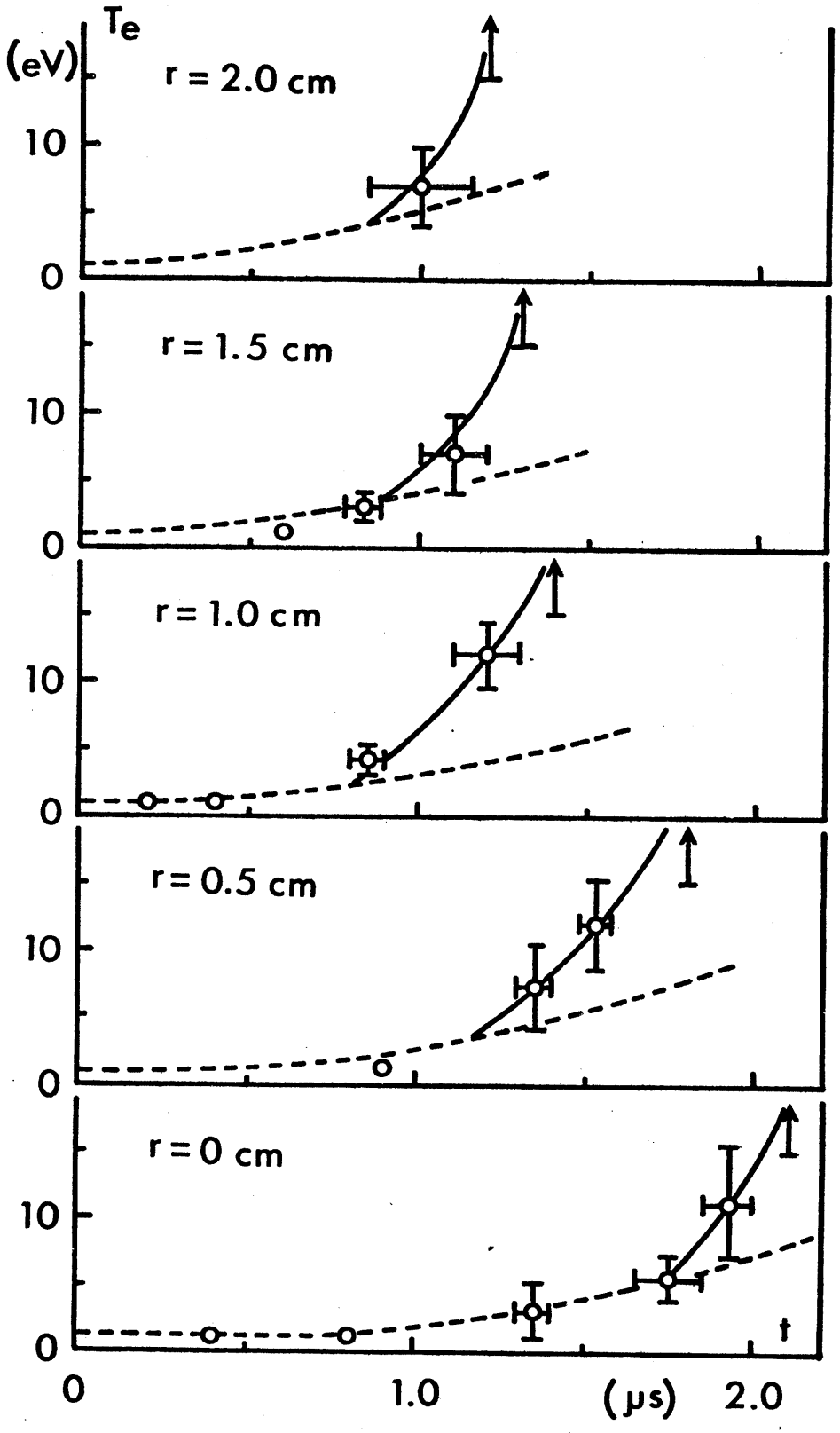

Fig.8

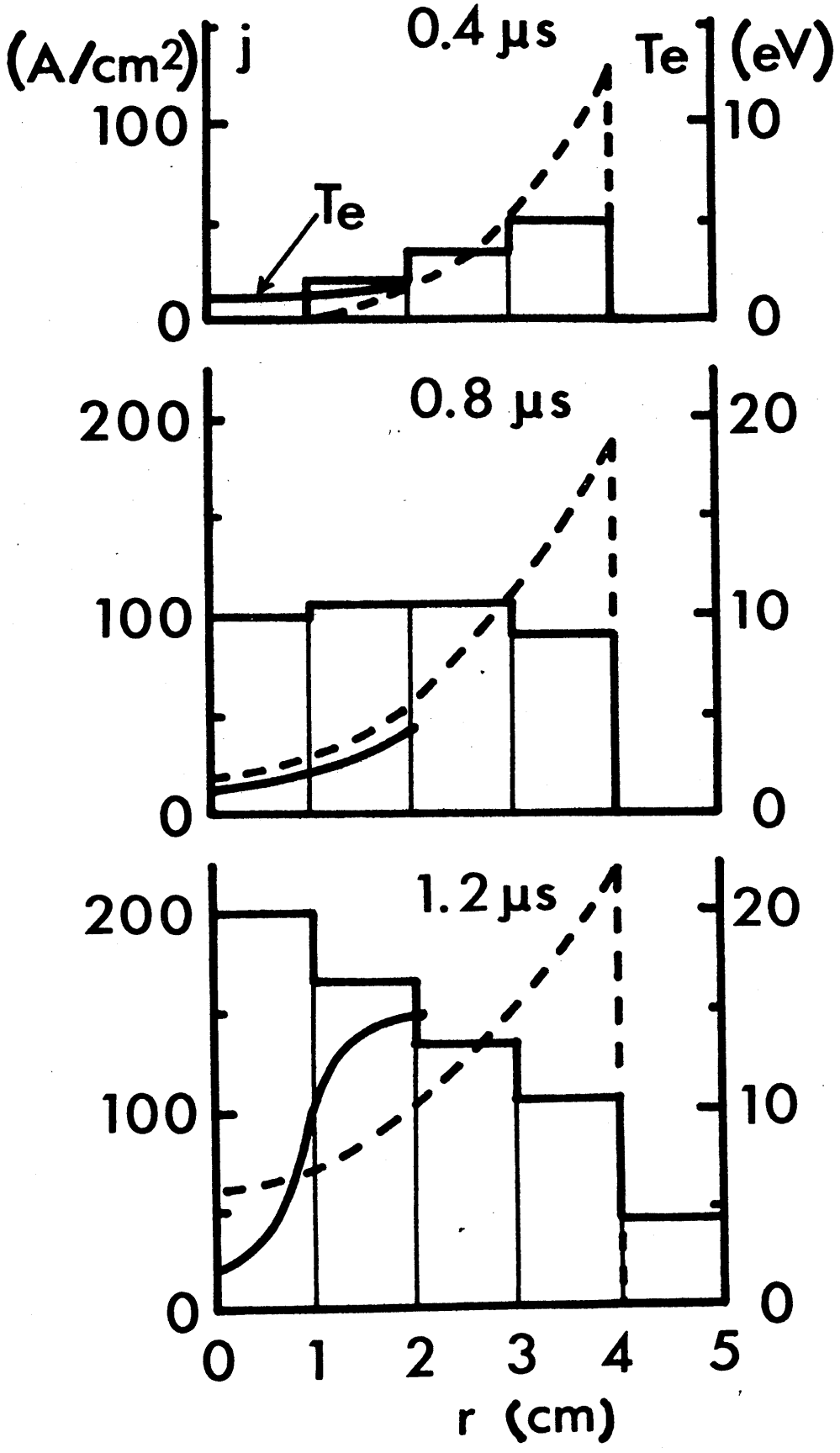
(A/cm2)
j
0.4 μs
Te
(eV)
100
10
Te
0
0
200
0.8 μs
20
100
10
0
0
200
1.2 μs
20
100
10
0
0
0 1 2 3 4 5
r (cm)

Fig. 9